



A Novel Low Temperature Transcutaneous Energy Transfer System Suitable for High Power Implantable Medical Devices: Performance and Validation in Sheep

*Thushari D. Dissanayake, *†David M. Budgett, ‡Patrick Hu, §Laura Bennet, ¶Susan Pyner, §Lindsea Booth, **Satya Amirapu, *‡Yanzhen Wu, and †§Simon C. Malpas

*Auckland Bioengineering Institute; ‡Department of Electrical and Computer Engineering; §Department of Physiology; **Department of Anatomy, University of Auckland, Auckland, New Zealand; ¶School of Biological & Biomedical Sciences, University of Durham, Durham, United Kingdom; and †Tetcor, Auckland, New Zealand

Abstract: Transcutaneous energy transfer (TET) systems use magnetic fields to transfer power across the skin without direct electrical connectivity. This offers the prospect of lifetime operation and overcomes risk of infection associated with wires passing through the skin. Previous attempts at this technology have not proved suitable due to poor efficiency, large size, or tissue damage. We have developed a novel approach utilizing frequency control that allows for wide tolerance in the alignment between internal and external coils for coupling variations of 10 to 20 mm, and relatively small size (50 mm diameter, 5 mm thickness). Using a sheep experimental model, the secondary coil was implanted under the skin in six sheep, and the system was operated to deliver a stable power output to a 15 W load

continuously over 4 weeks. The maximum surface temperature of the secondary coil increased by a mean value of $3.4 \pm 0.4^\circ\text{C}$ ($\pm\text{SEM}$). The highest absolute mean temperature was 38.3°C . The mean temperature rise 20 mm from the secondary coil was $0.8 \pm 0.1^\circ\text{C}$. The efficiency of the system exceeded 80% across a wide range of coil orientations. Histological analysis revealed no evidence of tissue necrosis or damage after four weeks of operation. We conclude that this technology is able to offer robust transfer of power to implantable devices without excess heating causing tissue damage. **Key Words:** Artificial hearts—Inductive power—Magnetic field—Transcutaneous energy transfer—Ventricular assist device—Wireless power.

An estimated 15 000 cardiac patients become potential candidates for implantation of circulatory assist devices, such as artificial hearts or ventricular assist devices, every year (1). Smart implantable biomedical devices such as these require high power levels that cannot be sustained by an implantable battery. Presently, this energy is provided by percutaneous leads. However, the use of percutaneous leads introduces an infection risk due to wires passing through the skin. Indeed, the REMATCH trial esti-

mated that 40% of left ventricular assist device (LVAD) complications were infection related (2). More recently, the INTERMACS registry indicated that infection remains the most common adverse event associated with artificial heart transplantation, with four times the incidence of infection compared to pump malfunction (3). One possible means to overcome the risk of infection associated with wires passing through the skin is via transcutaneous energy transfer (TET).

TET uses magnetic fields to transfer power from outside to inside the body without direct electrical connectivity. The basic structure of a TET system is illustrated in Fig. 1. The primary and the secondary coils of the system are separated by the patient's skin. In a generalized TET system, a battery pack supplies energy to an external TET controller, which generates

doi:10.1111/j.1525-1594.2009.00992.x

Received June 2009; revised November 2009.

Address correspondence and reprint requests to Dr. David Budgett, Auckland Bioengineering Institute, University of Auckland, UniServices House, Level 6, 70 Symonds Street, Auckland 1010, New Zealand. E-mail: d.budgett@auckland.ac.nz

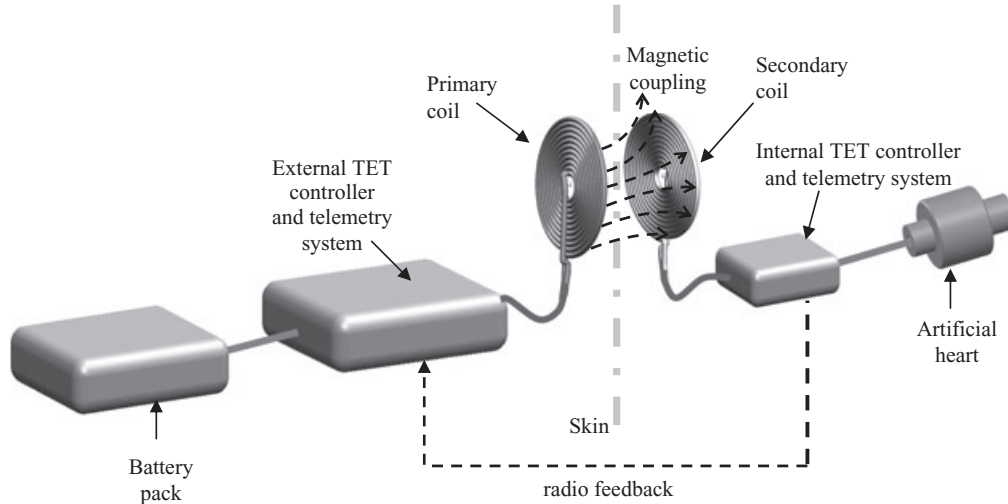


FIG. 1. Basic structure of a transcutaneous energy transfer (TET) system.

an AC sinusoidal waveform across the primary coil. The current in the primary coil produces a magnetic field that passes through the tissue of the body and induces current in the secondary coil. The induced AC voltage in the secondary coil is then rectified using an internal TET controller to a DC voltage, and this is supplied to the artificial heart. The system also has wireless telemetry to provide feedback to enable regulation of power to the biomedical device.

In the present study, we have developed a novel, high-power TET system that utilizes a closed loop frequency based controller to regulate the power delivered to a load under variable coupling conditions. We present temperature and histological profiles from tissue surrounding the devices implanted in adult sheep, in which up to 15 W of power was transferred continuously for 4 weeks.

MATERIALS AND METHODS

TET description

A simplified block diagram of the architecture of the overall TET system discussed in this paper is illustrated in Fig. 2. The primary coil is located outside the body and generates an electromagnetic field. This time varying magnetic field penetrates the skin and induces currents and voltages in the implanted secondary coil that can be used to derive power for the biomedical device. The TET system was designed to deliver power in the range of 5 to 25 W with a closed loop frequency based controller. With reference to Fig. 2, a DC voltage was supplied to the system with an external power supply. A current fed push-pull resonant converter was used to generate a high-frequency sinusoidal current across the

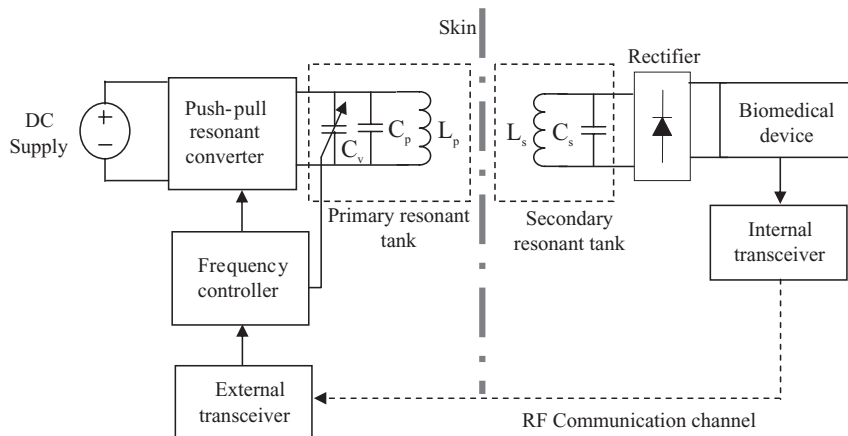


FIG. 2. The overall architecture of the developed TET, where L_p corresponds to primary coil; C_p and C_v corresponds to primary capacitor and variable capacitor, respectively; L_s corresponds to secondary coil; and C_s corresponds to secondary capacitor.

primary coil. Zero voltage and zero current switching were used to produce high efficiency, and the waveform has low harmonic distortion. The magnetic coupling between the primary and the secondary systems induces a sinusoidal voltage in the secondary coil which was rectified by the power conditioning circuit in the pickup to provide a stable DC output to the implanted load. Two nRF24E1 Nordic transceivers were used for wireless telemetry data communication. The DC output voltage of the pickup was detected and transmitted to the external transceiver. The output voltage to the load was regulated at 12 V to provide 15 W to the biomedical load. A resistive load was used to represent the biomedical device. The response time of this system was approximately 180 ms.

The power transfer of a TET system is dependent on resonant circuits at both the primary and secondary sides, which compensate for low magnetic coupling between the external and the internal coil. Normally, both primary and secondary coils are tuned to a fixed frequency. However, in this study, the operating frequency of the primary power converter is varied to regulate the power delivered to the implantable load and compensate for dynamic changes in coupling conditions. The frequency of the secondary resonant tank is governed by the fixed parameters C_s and L_s , as shown in Fig. 2; however, the frequency of the primary resonant tank is influenced by the parameters L_p , C_p , and C_v , where C_v is a variable capacitance specifically designed to adjust the resonant frequency. This variable capacitance is achieved using the switched capacitor control method described in Ping et al. (4). This involves switching a fixed capacitor in each resonant period using semiconductor devices. By varying the duty cycle of the switching devices, the average charging and discharging period of the capacitor is changed; thus, the effective capacitance of the fixed capacitor can be varied from zero to the full value of the fixed capacitor. In this implementation, the range of frequency is from 155 kHz ($C_v = 28\text{nF}$) to 178 kHz ($C_v = 0\text{nF}$) in the primary power converter. The secondary resonant tank was tuned to a fixed frequency of approximately 178 kHz. When C_v is 0nF, the primary resonant tank is fully tuned, and when the C_v is 28nF, the primary resonant tank is completely detuned. For this variation in frequency the system is able to regulate the output voltage at 12 V to tolerate load variations of 6–15 W at 20-mm axially aligned coil separation, and 15–24 W at 10-mm axially aligned coil separation.

The primary and secondary coils of the TET system were 50 mm in diameter with a primary coil

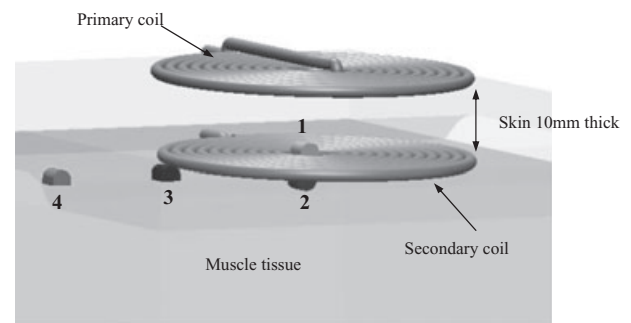


FIG. 3. Positioning of the sensors around the secondary coil: 1. front of secondary corresponds to the sensor place just under the skin above the secondary coil, 2. back of secondary placed under the secondary coil against the muscle, 3. side of secondary placed on the outer rim of the secondary coil, 4. 20 mm from secondary placed 20 mm from the outer rim of the secondary coil.

inductance of 12 μH and a secondary coil inductance of 3 μH . The weight of the primary and the secondary coils were 40 and 21 g, respectively. The frequency controller was designed to be capable of regulating power for coupling variations between 0.079 and 0.23, which corresponds to axially aligned separations of 20 to 10 mm between the primary and the secondary coils described earlier.

Both internal and external coils and the resonant capacitors were Parylene coated and encapsulated with medical grade silicon to provide a biocompatible barrier between the components and the body. Temperature sensors (Betatherm 10K3A1B thermistors) were attached to the primary and the secondary coil for measurement of temperature distribution around the coils. Figure 3 shows the placement of the temperature sensors around the secondary coil. Sensors 1 and 2 were placed at the front and back of the secondary coil, sensor 3 on the edge, and sensor 4 was 20 mm away from the edge of the coil. The temperature sensors were calibrated against a high precision Negative Temperature Coefficient (NTC) Resistive Temperature Device (RTD) (US sensor PPG101A1100 Ω RTD) immersed in a water bath with the power transfer system both active and turned off. The temperature sensors used for monitoring were 10 k Ω NTC thermistors with a resistance tolerance of $\pm 0.5\%$ (equivalent tolerance of $\pm 0.1^\circ\text{C}$). An Agilent 34970A data acquisition unit and LabView 8.5 software was used to acquire temperature data at one sample per minute.

Experimental preparation

All procedures were approved by the Animal Ethics Committee of The University of Auckland. Six female Romney/Suffolk sheep aged between 2 and 3

years and weighing an average of 57 kg were instrumented. Food, but not water, was withdrawn 18 h before surgery. Ewes were given 5 mL of Streptocin (procaine penicillin (250 000 IU/mL) and dihydrostreptomycin (250 mg/mL; Stockguard Laboratories Ltd, Hamilton, New Zealand) intramuscularly for prophylaxis 30 min prior to the start of surgery. Anesthesia was induced by intravenous (i.v.) injection of Alfaxan (alphaxalone, 3 mg/kg, Jurox, Rutherford, Australia), and general anesthesia was maintained using 2–3% isoflurane in O₂. Ewes were allowed to breathe spontaneously.

All surgical procedures were performed using sterile techniques (5). The back and flank of each sheep was closely shaved. An incision approximately 13 cm long was made in a dorsal to ventral direction approximately over the bottom rib. A subcutaneous pocket approximately 30 cm long was made and the secondary coil was advanced to the end of the pocket. Similarly, another control coil was also implanted on the contra-lateral side of sheep in order to compare the tissue samples between the active and inactive regions. The leads from the secondary coil and thermistors exited through the incision point and were sutured in place. The primary exterior coil was held in place over the subcutaneous coil through the use of elastic ties through the skin using a coil holder. No magnets, skin adhesive, or external pressure was applied to force the two coils together; thus, the primary coil was merely kept over the general region of the secondary coil. The long saphenous vein was catheterized to provide access for postoperative care and euthanasia. Postoperatively, the sheep received a 3-day prophylactic course of engemycin antibiotic (10 mg/Kg every 24 h of oxytetracycline, Intervet Ltd, Upper Hutt, New Zealand).

Following surgery, sheep were housed in separate metabolic cages with unrestricted access to water and food. They were kept in a temperature-controlled room ($16 \pm 1^\circ\text{C}$, humidity $50 \pm 10\%$), in a 12 h light/dark cycle. The venous catheter was kept patent by periodic flushing with heparinized isotonic saline.

Experimental design

After a 24 h period of equilibration, the circuit was activated and then was run continuously for 4 weeks with closed loop frequency regulation delivering 15 W to the load. During the 4-week period, temperature, output power, input current, and frequency in the primary power converter were measured. The secondary load was kept external to the sheep. The heat dissipated by the load was not contributing to the heat dissipated by the power transfer of the TET system. At the end of the 4-week period, the circuit

was turned off for 24 h and the equilibration temperature profiles around the surrounding tissue were recorded. At the end of the experiment, an autopsy was carried out on the animals, where 10×10 mm skin samples were excised from the area immediately above the secondary coil, as well as the contra-lateral control side. The tissue samples were embedded in paraffin, then 5 μm sections were cut. The resultant sections were stained using the hematoxylin and eosin method (H&E).

RESULTS

Power transfer capability

In each animal, 15 W of power transfer was successfully maintained for the 4-week period. Power ranged from 14.6–15.1 W on average in the six sheep. There were short intervals in which the power delivered dropped below 15 W. The maximum time period when the power was below 14.5 W was a total of 26 min over the 4-week period. The cause of inadequate power delivery is due to poor alignment between the two coils—this was attributed to the general behavior of each sheep; that is, as they moved from sitting to standing or twisted their bodies so the orientation between the primary and the secondary coils altered. As noted in the methods section, while the animals were within metabolic cages that prevented them turning around completely, they were allowed relatively free movement. Unless the power transfer dropped below 12 W, we did not manually alter the primary coil position.

The coupling variation between the primary and the secondary coil over 24 h in a single animal is shown in Fig. 4 in terms of coupling coefficient k , the corresponding axially aligned separation, observed variation in frequency, and the power delivered to the load. The variation in frequency corresponds to variation in coupling between the primary and the secondary coils due to the physical movement of the sheep. The variation in frequency was measured, and the corresponding change in coupling was inferred from bench tests that established the relationship between the two parameters prior to implantation. Frequency variation was between 156.5 and 185.4 kHz, and the corresponding coupling coefficient varied between 0.045 and 0.23, which is equivalent to an axial aligned separation variation of 23–10 mm. The short intervals of less than 15 W correspond to intervals where the coupling has been too low for the controller to compensate.

Temperature changes

For all sheep, the steady state was reached within 20–30 min from the initial baseline temperature. The

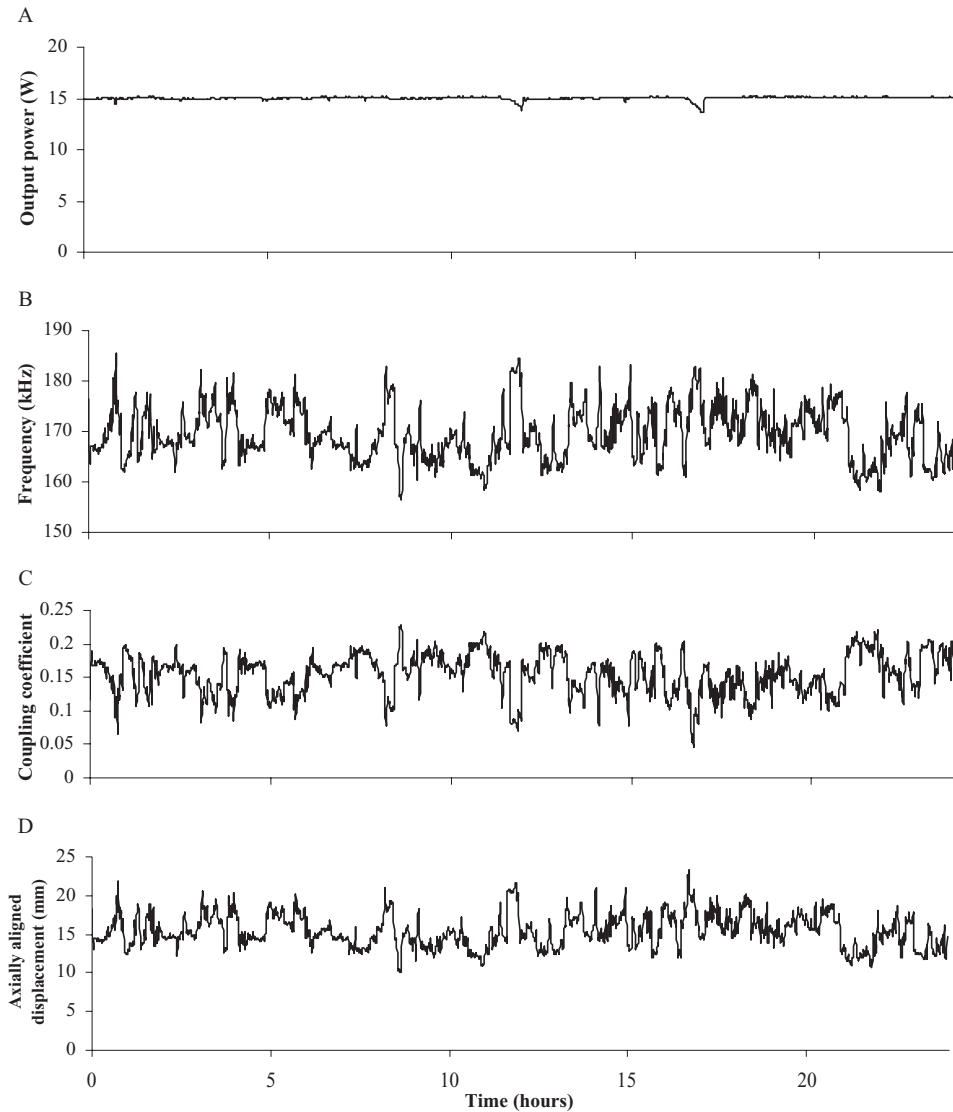


FIG. 4. Power delivered over 24 h in one sheep (A) with the corresponding frequency variation (B) over the same period of time, the equivalent coupling coefficient (C), and axially aligned separation (D).

maximum temperature rise (3.9°C) above a baseline of 34.1°C was recorded in the sensor placed at the center of the secondary coil under the skin (Fig. 5). The average temperature rise over the 4-week period was $3.4 \pm 0.4^{\circ}\text{C}$ (mean \pm SEM) (Table 1) and the average absolute temperature over this period was $37.7 \pm 0.3^{\circ}\text{C}$ (mean \pm SEM) in the six animals. To some extent, it is likely that the temperature rise under the skin is also affected by the heat radiated from the primary coil, where the maximum temperature rise was 12.9°C , above a base line of 28.0°C . This temperature did not exceed 41.0°C in any sheep.

On the back side of the secondary coil, that is, the side facing the muscle, the average temperature rise

over 4 weeks was $1.5 \pm 0.3^{\circ}\text{C}$. This temperature was relatively stable within each animal. The average temperature rise on the outer rim of the secondary coil was $1.4 \pm 0.1^{\circ}\text{C}$. The average temperature 20 mm from the secondary coil was $0.8 \pm 0.1^{\circ}\text{C}$. Thus, overall, the rise in temperature was very much localized to the center of the secondary coil.

The TET system was run for 1 h with 25 W of power being delivered to the load in one sheep, and a mean temperature rise of 5.1°C was observed on the sensor placed at the center of the secondary coil directly under the skin (sensor 1). A power level of 15 W was chosen for a long-term trial because it is expected to cover the power demands of a LVAD device.

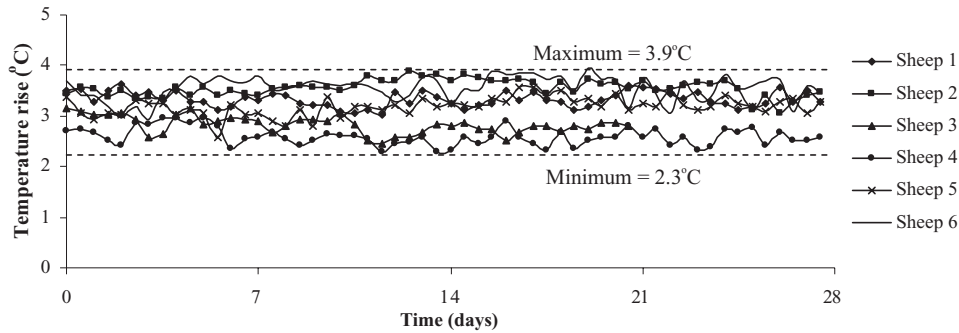


FIG. 5. Temperature rise of the sensor placed above the secondary coil under the skin over 28 days for six different sheep when delivering 15 W of power to the load.

Histology

The H&E stain clearly distinguished the basophilic (purple) and eosinophilic (red) structures within the tissue section (Fig. 6). A comparison between active (temperature elevated coil side) and inactive (contralateral coil side with no temperature elevation) skin samples indicated no evidence for tissue necrosis, apoptosis, or edema. A more detailed examination at increasing magnification (low to high), confirmed cell membrane and nuclei integrity (Fig. 6C,F). Furthermore, the dermal layers within each sample remained intact and clearly distinguishable (Fig. 6A,D); this was also the case for hair follicle and melanocyte structural composition (Fig. 6B,E).

DISCUSSION

We have developed a new TET system tolerant to large movements of the primary coil with respect to the secondary coil without disrupting power transfer. We illustrate the ability to deliver 15 W of power with low increases in temperature around the secondary coil, and histological analysis of the skin revealed no discernible evidence of tissue damage.

Previous attempts at TET technology appear to have been compromised by either poor efficiency, large size, thermally induced tissue damage, or tissue damage caused by frictional forces between the magnets (6). Early work carried out by Schuder has shown theoretical power efficiencies of up to 95% at

50–69 W power transmission; however, the coils used in these analysis are 100 mm in diameter (7). The Thermedics TET system was reported to have efficiencies varying from 65 to 80%. In this system, the geometry of the secondary coil was configured to create a shallow mould rising above the plane of the secondary coil (8). A recent development of a TET system designed by the New Energy and Industrial Development Organization artificial heart project reports a maximum transmission efficiency of 87.3%. This system consists of an internal coil with a 53 mm external diameter (with a height of 9 mm), and also consists of a 38-mm diameter ferrite core. Rather than a flat coil, the coil is shaped in an oval, which would present a significant bulge when placed under the skin. The external diameter of the primary coil is 92 mm in diameter. Both these coils are considerably larger in size compared to the coils that we have designed. Furthermore, at 20 W power transmission, the maximum surface temperature of the internal coil is 46.1°C, and this was measured at the ferrite core (9). This high temperature is a major disadvantage of the use of ferrites in the system. Although ferrites offer the opportunity of improved magnetic coupling, it comes at the expense of added weight and increasing core losses and temperature rises. We have demonstrated that with good controller characteristics, air core coils can be used to provide a compact, lightweight set of internal and external coils. The

TABLE 1. Temperature distribution around the secondary coil over 28 days, data shown as mean \pm SEM of temperature rise and absolute temperature at different locations for six sheep

Location	Baseline temperature (°C)	Mean rise \pm SEM (°C)	Absolute mean \pm SEM (°C)
Front of secondary coil under the skin	34.1 \pm 0.3	3.4 \pm 0.4	37.7 \pm 0.3
Back of secondary coil on the muscle side	36.9 \pm 0.3	1.5 \pm 0.3	38.3 \pm 0.3
Side of secondary coil	34.9 \pm 0.1	1.4 \pm 0.1	36.3 \pm 0.1
20 mm from the secondary coil	34.9 \pm 0.2	0.8 \pm 0.1	35.8 \pm 0.2

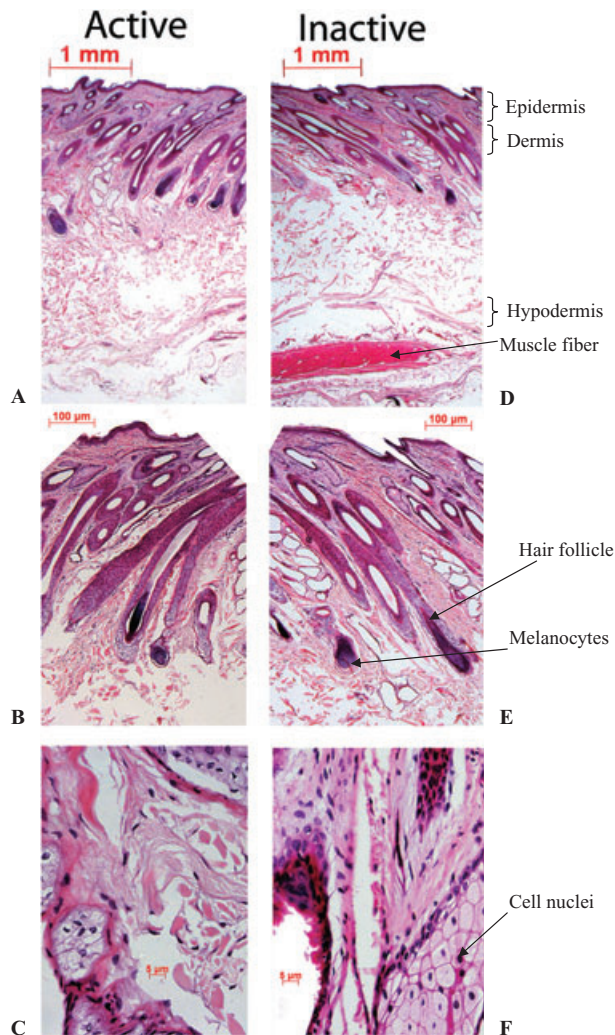


FIG. 6. Examples of skin tissue stained with H&E from the active (A–C) and inactive (D–F) sites. For both sets of conditions, the dermal layers show no evidence of edema, necrosis, or apoptosis (A,D). Hair follicles and melanocytes are readily identifiable again with no apparent change in morphology (B,E). Cell membranes and nuclei have retained structural integrity (C,F)

maximum power efficiency of the frequency controlled system was 82% when delivering 15 W of power to the load.

TET systems have been used in the AbioCor total artificial heart from Abiomed and the Arrow Lion-Heart LVAD. The AbioCor TET system performs with an efficiency ranging from 68 to 72% for coil separations between 3 mm and 10 mm (10,11). The LionHeart system requires a minimum of 14 W, and the system also contains an internal rechargeable battery that allows for 20 min of operational time without the TET system (12). The HeartSaver TET system designed by Mussivand et al. consists of a primary coil measuring 58 mm in diameter by 30 mm in height and weighing 75 g, and the secondary

implanted coil measuring 70 mm in diameter by 20 mm in height, and weighing 125 g. It demonstrates a power efficiency of 60–80% for power demands of 5–70 W (13). The primary and secondary coils that were designed for the presented system were smaller in size, lighter in weight, and tolerant to misalignment without heavily compromising power efficiency compared to previously developed TET systems (13).

Previous research on thermal effects of skin tissue has shown that tissue damage occurs when the local tissue temperature reaches 42°C (14). In our study, at no time did the internal temperature exceed 39.6°C in any situation. Even lower secondary coil temperatures could be achieved through the use of a larger secondary coil. The maximum temperature reached in our experimental setup for the primary coil was 41°C when delivering 15 W to the load. This elevated temperature applied to the surface of the skin appeared to have no detrimental effect to the structural integrity of the skin (see Fig. 6). However, we cannot rule out the possibility that a longer exposure to an elevated temperature may cause structural damage. An earlier performance evaluation of a TET system using a porcine model by Mussivand et al. (13) demonstrated no adverse effects to tissue when up to 40 W of power was delivered to an implanted load without the tissue contacting surface on the implanted coil exceeding 42°C. In our TET study, no attempt was made to reduce the conduction of heat from the primary coil into the body. Given the high tolerance to coil separation, it would be feasible to insulate the primary coil from the skin surface to lower the temperature observed at the hottest thermistor.

CONCLUSION

Our variable frequency TET system is capable of delivering regulated power to an implantable medical device without heating tissue above a mean temperature of 38.3°C. Delivering 15 W over a period of 4 weeks caused no apparent damage to the surrounding tissue or irritation at the skin surface. Efficiency exceeds 80%, and compact 50 mm diameter coils can be misaligned with respect to each other by as much as ± 20 mm without compromising full power transfer. This TET system offers a patient-friendly, highly reliable power delivery system for an implanted heart pump—eliminating the risk of driveline infections.

REFERENCES

1. Zhao L, Foo CF, Tseng KJ. A new structure transcutaneous transformer for artificial heart system. *IEEE Trans Magn* 1999;35:3550–2.

2. Milano CA, Lodge AJ, Blue LJ, et al. Left ventricular assist devices: new hope for patients with end stage heart failure. *N C Med J* 2006;67:110–5.
3. Holman W, Kirklin J, Naftel D, et al. Early infections after MCS/D implant in 455 patients: incidence, location and outcome. *J Heart Lung Transplant* 2009;28:S155–S155.
4. Ping S, Hu AP, Malpas S, Budgett D. *A frequency control method for regulating wireless power to implantable devices*. IEEE ICIEA conference, Harbin, China, 2007.
5. Bennet L, Roelfsema V, Dean J, et al. Regulation of cytochrome oxidase redox state during umbilical cord occlusion in preterm fetal sheep. *Am J Physiol Regul Integr Comp Physiol* 2007;292:R1569–76.
6. Nishimura TH, Eguchi T, Hirachi K, Maejima Y, Kuwana K. *A large airgap flat transformer for a transcutaneous energy transfer transmission system*. In 25th IEEE Power Electronics Specialists Conference. pp. 1323–9; 1994.
7. Schuder JC. Powering an artificial heart: birth of the inductively coupled-radio frequency system in 1960. *Artif Organs* 2002;26:909–15.
8. Szycher M, Clay W, Gernes D, Sherman C. Thermedics' approach to ventricular support systems. *J Biomater Appl* 1986;1:79–83.
9. Okamoto E, Yamamoto Y, Akasaka Y, Motomura T, Mitamura Y, Nosé Y. A transcutaneous energy transmission system with hybrid energy coils for driving an implantable biventricular assist device. *Artif Organs* 2009;33:622–6.
10. Zareba KM. The artificial heart—past, present, and future. *Med Sci Monitor* 2002;8:RA72–77
11. Mussivand T, Holmes KS, Hum A, Keon WJ. Transcutaneous energy transfer with voltage regulation for rotary blood pumps. *J Artificial Organs* 1996;20:621–4.
12. Culver DD, Khan MG, White WB. *Encyclopedia of Heart Diseases*. London: Academic Press, 2006.
13. Mussivand T, Miller JA, Santerre PJ, et al. Transcutaneous energy transfer system performance evaluation. *J Artif Organs* 1993;17:940–7.
14. Gowrishankar TR, Stewart DA, Martin GT, Weaver JC. Transport lattice models of heat transport in skin with spatially heterogeneous, temperature-dependent perfusion. *Bio Med Eng Online* 2004;3. Available at: <http://www.biomedical-engineering-online.com/content/3/1/42>